

## Polarons in Suspended Carbon Nanotubes

I. Snyman<sup>1,2,\*</sup> and Yu. V. Nazarov<sup>3</sup>

<sup>1</sup>National Institute for Theoretical Physics, Private Bag X1, 7602 Matieland, South Africa

<sup>2</sup>Department of Physics, Stellenbosch University, Private Bag X1, 7602 Matieland, South Africa

<sup>3</sup>Kavli Institute of Nanoscience, Delft University of Technology, 2628 CJ Delft, The Netherlands

(Received 15 April 2011; published 15 February 2012)

We prove theoretically the possibility of electric-field controlled polaron formation involving flexural (bending) modes in suspended carbon nanotubes. Upon increasing the field, the ground state of the system with a single extra electron undergoes a first-order phase transition between an extended state and a localized polaron state. For a common experimental setup, the threshold electric field is only of the order of  $\approx 5 \times 10^{-2} \text{ V}/\mu\text{m}$ .

DOI: 10.1103/PhysRevLett.108.076805

PACS numbers: 73.63.Fg, 62.25.-g, 71.38.-k

Because of their unique material properties, carbon nanotubes make ideal flexible nanorods for mechanical applications [1]. Coupling their mechanical motion to electronic degrees of freedom leads to nonlinear dynamics [2]. Current technology [3] allows for the fabrication of ultraclean nanotubes in which electrons propagate ballistically [4] rather than diffusively. In combination with a high quality factor [5], this allows for resonant excitation and coherent manipulation of discrete degrees of freedom. The envisioned devices may find application in quantum information processing.

In current devices, a discrete spectrum is obtained by embedding a quantum dot on a suspended nanotube [2,3]. In this Letter, we prove the possibility of the controllable formation of discrete states of a different kind, namely, polarons. A polaron is an electron localized inside a lattice deformation that the electron itself produces. Our setup is shown in Fig. 1. It consists of an ultraclean semiconducting single wall carbon nanotube cantilever. The setup is similar to the nanorelay proposed in Ref. [6] and to the experimental setup of Ref. [7] but operated in a different regime, namely, that of a single electron on the cantilever. This is achieved by putting the Fermi energy of the tube just below the energy of the bottom of the conduction band. The Fermi energy is tuned by adjusting the voltage bias on the metallic electrode A in Fig. 1.

If the electron enters the suspended part of the tube, it experiences a force  $\mathbf{F} = -e\mathbf{E}$ . The electric field  $\mathbf{E}$  may be due to an external source or to the image charge induced by the electron in the substrate below the cantilever. The force  $\mathbf{F}$  deforms the tube. As a result, the potential energy of the electron is lowered. Thus, the tube deformation produces a potential well that may trap the electron.

This allows for unprecedented manipulation possibilities. One can, for instance, envisage the coherent manipulation of the quantum state of the polaron by the excitation (with a high frequency source) of the tube's flexural modes. These possibilities are present neither for the well-studied polarons in bulk solids [8] nor for previously studied

polarons in carbon nanotubes [9] that originate from axial stretching and radial bending modes of the tube rather than from macroscopic flexural modes.

Our main results are contained in Fig. 2. At small electric fields, the ground state consists of an undeformed tube without a polaron. As the field is increased beyond a critical value, the system undergoes a first-order phase transition to a localized polaron state. For realistic values of a suspended tube length  $L = 1 \mu\text{m}$  and tube radius  $r = 1 \text{ nm}$ , the threshold electric field is  $0.051 \text{ V}/\mu\text{m}$ , and the tip deviation is  $0.89 \text{ nm}$ . This is the field that would be produced by an image charge induced in a metallic substrate  $0.12 \mu\text{m}$  below the tube.

The typical energy scale for the polaron state is set by the electron confinement energy  $\varepsilon_e = \hbar^2/2m^*L^2$ , where  $m^*$  is the effective electron mass. The ratio  $\hbar\omega_0/\varepsilon_e$ , where  $\omega_0$  is the frequency of the lowest flexural mode of the tube, is small: It equals  $0.0332$ , independent of  $r$  or  $L$ . We therefore neglect the zero point motion (associated with energy  $\hbar\omega_0$ ) of the cantilever and treat its displacement as a classical variable.

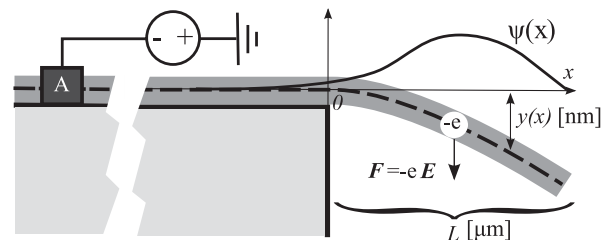


FIG. 1. Setup: A semiconducting single wall carbon nanotube cantilever of length  $L$ . The supported part of the tube rests on an insulating substrate. The voltage-biased metallic electrode A is connected to the supported part of the tube by means of a tunnel barrier. An electron that enters the suspended part of the tube experiences a force  $\mathbf{F} = -e\mathbf{E}$  perpendicular to the tube. As a result, the tube is deformed so that each point  $x$  on the tube undergoes a displacement  $y(x)$  perpendicular to the  $x$  axis. The electron wave function  $\psi(x)$  is also indicated.

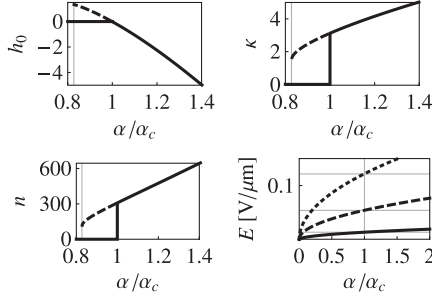


FIG. 2. Results of the numerical calculation: In the top panels and in the bottom left panel, solid curves indicate ground state properties. Dashed curves indicate properties of the metastable polaron state. A thin vertical line indicates the value of  $\alpha/\alpha_c$  below which no polaron solutions exist. The critical value of  $\alpha$  is  $\alpha_c = 312.03$ . Top left: The minimal values  $h_0$  of the (dimensionless) energy  $h[\phi, f]$  [cf. Eq. (2)] vs  $\alpha/\alpha_c$ . Top right: The dimensionless inverse localization length  $\kappa$  vs  $\alpha/\alpha_c$ . Bottom left: The ratio  $n = U/\hbar\omega_0$  between the bending energy and the lowest phonon energy vs  $\alpha/\alpha_c$ . Bottom right: The electric field  $E$  as a function of  $\alpha/\alpha_c$ , for  $L = 1 \mu\text{m}$ , and three different tube radii  $r$ . Solid curve,  $r = 0.5 \text{ nm}$ ; dashed curve,  $r = 1 \text{ nm}$ ; and dotted curve,  $r = 1.5 \text{ nm}$ .

We neglect the van der Waals force exerted on the suspended part of the tube by the distant substrate. In the Supplemental Material [10], we identify the region of parameter space where this is a reasonable approximation.

The truncation of the carbon lattice at the suspended tip of the tube may lead to states localized at the tip, with energies in the gap between the valence and conduction bands [11]. An electron in such a state is virtually unaffected by the deformation of the tube and, hence, cannot form a polaron. The polaron we consider is formed by an electron coming from the delocalized states at the bottom of the conduction band. If localized tip states with energies in the gap are present, they are filled before the states involved in polaron formation come into play. The presence of occupied localized states may lead to an uncompensated charge on the tip. In the main text, we consider the common situation where no localized states are present [11] or their charge is neutralized by adsorbing charged impurities at the tip. In the Supplemental Material [10], we analyze what happens in the absence of such neutralizing impurities, concluding that polaron formation still occurs, albeit at larger electric fields.

The supported part of the tube is tightly clamped to the substrate by van der Waals forces and cannot be deformed. We choose a coordinate system as indicated in Fig. 1. The system is described by two fields, namely, the tube profile  $y(x)$  and the wave function  $\psi(x)$  of the single electron in the conduction band, which can be taken as real and is normalized. We assume small deflections in the sense that  $\max\{|y(x)|\} \ll L$ .

The ground state configuration is obtained by minimizing the energy functional

$$H[\psi, y] = \int_{-\infty}^L dx \underbrace{\frac{\hbar^2}{2m^*} (\partial_x \psi)^2}_{=T} + \underbrace{eEy\psi^2}_{=V} + \underbrace{\frac{YI}{2} (\partial_x^2 y)^2}_{=U}. \quad (1)$$

The boundary conditions on the tube profile are  $y(x \leq 0) = y'(x \leq 0) = 0$  and  $y''(L) = y'''(L) = 0$ . The boundary conditions on the wave function are  $\psi(-\infty) = \psi(L) = 0$ .

The term  $T$  is the kinetic energy of the electron. The effective mass  $m^*$  is inversely proportional to the radius  $r$  of the nanotube [12]:  $m^* = 0.6m_e a_0/r$ , where  $m_e$  is the true electron mass and  $a_0$  is the Bohr radius. In the Supplemental Material [10], we derive the kinetic term as well as the vanishing boundary condition at the tip, starting from the Dirac Hamiltonian that describes electron dynamics close to the bottom of the tube's conduction band.

If the electron is at position  $x$  in the suspended part of the tube, it has undergone a vertical displacement  $y(x)$  in the direction of the electrostatic force  $-eE$ . This means that the electron sees a potential well with the same profile as the tube. The term  $V$  in Eq. (1) accounts for this.

The term  $U$  is the elastic energy of the deformed tube [13]. In the small deflection approximation, the energy stored in stretching modes is smaller than the energy stored in flexural modes by a factor of the order of  $[y(L)/L]^2 \ll 1$ . We therefore take only bending energy into account.  $Y = 1.2 \times 10^{12}$  is the tube's Young's modulus [14].  $I \approx \pi g r^3$  is the second moment of area of the tube cross section. Here  $g = 6.4a_0$  is the thickness of the cylinder wall of the nanotube [14].

We introduce dimensionless quantities  $h = \frac{2m^*L^2}{\hbar^2} H$ ,  $\phi = \sqrt{L}\psi$ ,  $f = \frac{YI}{eEL^3} y$ , and  $z = x/L$ . The dimensionless energy functional

$$h[\phi, f] = \int_{-\infty}^1 dz (\partial_z \phi)^2 + \alpha \left[ f\phi^2 + \frac{1}{2} (\partial_z^2 f)^2 \right] \quad (2)$$

depends on a single parameter, the dimensionless coupling constant  $\alpha = 2m^*(eE)^2L^5/\hbar^2YI$ .

Two classes of solutions, or phases, can be distinguished. The first comprises extended electronic states, in which the magnitude of the wave function is sizable over the whole length of the tube. (We consider a tube with total length  $\gg L$ .) The average charge in the suspended part of the tube is vanishingly small. The force exerted on the tube by the electric field, and hence the deformation of the tube, is zero. The total energy of such a state is equal to the kinetic energy of the electron. The lowest extended state energy is zero, corresponding to an electron wave function with an infinite wavelength. The second class of states is of the polaron type. These consist of an electron trapped in the potential well associated with the tube deformation that the electron itself produces. The electron wave function  $\phi$

decays exponentially into the supported part of the tube, i.e.,  $\phi = \phi_0 e^{\kappa z}$  for  $z < 0$ , where  $\kappa$  is the inverse localization length. Because of the negative potential energy of the trapped electron, the total energy of the state can become negative. When this happens, the ground state of the system is of the polaron variety, since all extended states have positive energies. Otherwise, the polaron state is metastable, since there exists an extended state of zero energy.

We perform a variational calculation to determine into which of these two classes the ground state falls for a given value of  $\alpha$ . We approximate  $\phi$  and  $f$  as polynomials of degree  $M$  in the suspended part of the tube, i.e.,

$$\phi_{\text{var}}(z) = \begin{cases} \sum_{m=1}^M a_m (1-z)^m & \text{if } z \geq 0, \\ \left( \sum_{m=1}^M a_m \right) e^{\kappa z} & \text{if } z < 0, \end{cases} \quad (3)$$

$$f_{\text{var}}(z) = \begin{cases} \sum_{m=1}^M b_m z^{m+1} & \text{if } z \geq 0, \\ 0 & \text{if } z < 0. \end{cases} \quad (4)$$

The energy  $h_{\text{var}} = h[\phi_{\text{var}}, f_{\text{var}}]$  is then varied with respect to the  $a_m$ ,  $b_m$ , and  $\kappa$ , subject to the constraints that  $\phi$  is normalized and that its derivative is continuous at  $z = 0$ .

In Fig. 3, the (dimensionless) energy  $h_{\text{var}}$ , minimized with respect to  $a_m$  and  $b_m$  is plotted as a function of  $\kappa$  for various values of the coupling constant  $\alpha$ . The calculation was performed with  $M = 7$ . For given  $\alpha$ , the polaron state, if it exists, is associated with a minimum at  $\kappa > 0$  of the corresponding curve. If the polaron minimum has an

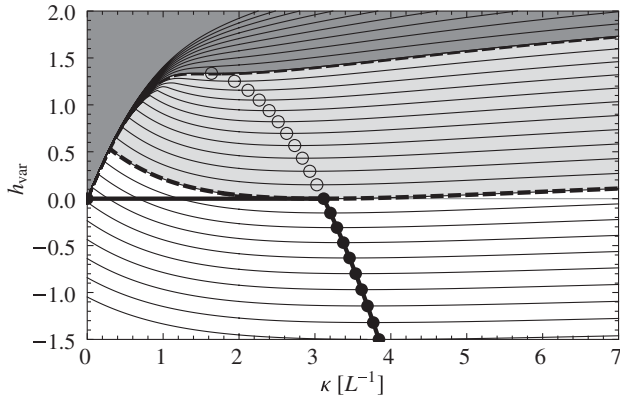


FIG. 3. First-order phase transition: The dimensionless energy  $h_{\text{var}}$  minimized with respect to  $a_m$  and  $b_m$ , versus  $\kappa$ , for several values of the coupling constant  $\alpha$ . The bottommost curve corresponds to  $\alpha = 355.2$ . In each subsequent curve, the value of alpha is decremented by 4.797. The curves in the white region of the graph ( $\alpha > \alpha_c = 312.03$ ) have minima at  $\kappa > 0$  where the energy is negative (black dots). These minima correspond to a stable polaron ground state. Curves in the light gray region ( $\alpha_c > \alpha > \alpha_{\text{min}} = 258.96$ ) have local minima at  $\kappa > 0$  (open circles). These minima correspond to a metastable polaron state. For  $\alpha < \alpha_{\text{min}}$  (dark gray region), curves have no minimum at  $\kappa > 0$  and no polaron state exists.

energy that is negative (black dots in Fig. 3), the polaron is the stable ground state of the system. We obtain a critical value  $\alpha_c = 312.03$ . For  $\alpha < \alpha_c$ , the energy of the polaron minimum becomes positive, and the polaron state is metastable (open circles in Fig. 3). For  $\alpha < \alpha_{\text{min}} = 258.96$ , the curves of  $h_{\text{var}}$  versus  $\kappa$  no longer have a minimum at nonzero  $\kappa$ , and no polaron state exists. At  $\alpha = \alpha_c$ , we obtain a critical tip displacement  $f_c(1) = 0.138$ . For  $L = 1 \mu\text{m}$  and  $r = 1 \text{ nm}$ , this gives  $y_c(L) = 0.89 \text{ nm}$  and a critical electric field  $0.051 \text{ V}/\mu\text{m}$ . More detail about the variational calculation, as well as an alternative numerical calculation, can be found in the Supplemental Material [10].

We also calculate  $n = U/\hbar\omega_0$ , where  $U$  is the bending energy and  $\omega_0 = 3.52\sqrt{YI/\rho}/L^2$  [8] is the angular frequency of the lowest harmonic of the suspended tube. Here  $\rho = 0.674m_c r/a_0^2$  is the mass per unit length of the tube, and  $m_c$  is the mass of a carbon atom. The quantity  $n$ , being the ratio between the energy stored in the deformed tube and the energy of a single phonon, is an estimate of the number of phonons involved in the tube deformation. It depends only on  $\alpha$ , and not on  $L$  and  $r$  separately, as we show in the Supplemental Material [10]. In the lower left panel of Fig. 2,  $n$  is plotted as a function of  $\alpha$ . When the transition to the polaron state occurs, there are on the order of 300 phonons in the tube. The fact that  $n$  is large in the polaron state provides additional *a posteriori* justification for treating the tube deformation classically.

An important question to ask is whether values of  $\alpha$  that are of the order of  $\alpha_c$  and larger can be reached for realistic values of the length  $L$ , radius  $r$ , and external electric field  $E$ . Typical radii are of the order of 1 nm. Typical lengths are of the order of 1  $\mu\text{m}$ . In the bottom right panel of Fig. 2, we plot the electric field  $E$  versus the corresponding  $\alpha$  for  $L = 1 \mu\text{m}$  and three values of  $r$  ranging from 0.5 to 1.5 nm. We see that producing a coupling constant in excess of  $\alpha_c$  requires an electric field of  $0.013 \text{ V}/\mu\text{m}$  for the thinnest tubes and  $0.126 \text{ V}/\mu\text{m}$  for the thickest tubes. These are quite reasonable values and can be attained by placing the tube either inside a charged capacitor or above a metallic substrate. In the latter case, the electric field is due to the induced image charge in the substrate. To produce a field of  $0.126 \text{ V}/\mu\text{m}$ , the distance to the substrate must be  $0.076 \mu\text{m}$ , while for a field of  $0.013 \text{ V}/\mu\text{m}$ , it should be  $0.23 \mu\text{m}$ .

The above results focus on the regime of  $\alpha$  close to  $\alpha_c$ . It is also necessary to check whether realistic parameters allow for large enough  $\alpha$  that the polaron will not be destroyed by thermal fluctuations. If we assume a temperature of 10 mK [5], the thermal energy is  $10^{-3} \text{ meV}$ . For  $L = 1.2 \mu\text{m}$ ,  $r = 0.8 \text{ nm}$ , and  $E = 0.119 \text{ V}/\mu\text{m}$ , we find a polaron ground state energy  $-0.6 \text{ meV}$ , so that thermal fluctuations are 2 orders of magnitude too small to destroy the polaron state. The tip displacement is 14 nm, consistent with the assumption that  $y \ll L$ .

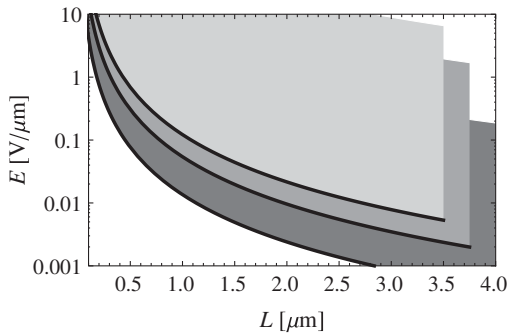


FIG. 4. Phase diagram: The three different shaded regions correspond to different tube radii. Dark gray,  $r = 0.5$  nm; gray,  $r = 1$  nm; and light gray,  $r = 1.5$  nm. In each case the shaded region indicates where the ground state is a polaron. At large  $L$ , the upper planes have been cut away to reveal the planes below. The lower boundaries (black curves) indicate the first-order transition where  $\alpha = \alpha_c$ . The upper boundaries correspond to  $y(L) = L$ .

It is informative to draw a phase diagram, indicating the region in parameter space where the ground state is of the polaron variety. There are two conditions that have to be met. First, as we have discussed above, the coupling constant must be large enough, i.e.,  $\alpha(r, L, E) > \alpha_c = 312.03$ . Second, the tube deflection must not become too large; otherwise, the tube will come in contact with the substrate. We take  $y(L) \sim L$  as the criterion for large deflection. (At this point the small deflection approximation, on which our analysis relied, also breaks down.) In the Supplemental Material, we derive the inequality involving  $E$ ,  $r$ , and  $L$  that is implied by  $y(L) < L$ . In Fig. 4, we show three cuts through the phase diagram in the  $E$ - $L$  plane, for  $r = 0.5$ , 1, and 1.5 nm, respectively. We see that the value of the largest allowed electric field is always several orders of magnitude larger than the smallest allowed electric field.

In conclusion, we found that at strong coupling (large  $\alpha$ ) the ground state of the system is a polaron. As the coupling is decreased beyond the critical value of  $\alpha_c = 312.03$ , a first-order phase transition occurs to an extended state. For realistic values  $L = 1$   $\mu\text{m}$  for the length of the suspended tube and  $r = 1$  nm for the tube radius, the critical tip displacement is 0.89 nm, and an electric field of 0.051 V/ $\mu\text{m}$  is required to realize the polaron phase. A field of this magnitude can be produced by an image charge in a metallic substrate 0.12  $\mu\text{m}$  below the cantilever. It can also be produced by placing the tube inside a charged capacitor.

In future work, we plan to study the nonlinear dynamics of a single polaron as well as the interaction between polarons in the same or adjacent suspended tubes. The eventual aim is to exploit the coupling between mechanical and electrical degrees of freedom for the coherent manipulation of the quantum state of the polaron.

This research was supported by the National Research Foundation (NRF) of South Africa.

\*isnyman@sun.ac.za

- [1] V. A. Popov, *Mater. Sci. Eng.*, R **43**, 61 (2004); K. L. Ekinci and M. L. Roukes, *Rev. Sci. Instrum.* **76**, 061101 (2005).
- [2] G. A. Steele, A. K. Hüttel, B. Witkamp, M. Poot, H. B. Meerwaldt, L. P. Kouwenhoven, and H. S. J. van Zant, *Science* **325**, 1103 (2009).
- [3] J. Gao, Q. Wang, and H. Dai, *Nature Mater.* **4**, 745 (2005). G. A. Steele, G. Götz, and L. P. Kouwenhoven, *Nature Nanotech.* **4**, 363 (2009).
- [4] M. R. Buitelaar, A. Bachtold, T. Nussbaumer, M. Iqbal, and C. Schönenberger, *Phys. Rev. Lett.* **88**, 156801 (2002); P. Jarillo-Herrero, J. Kong, H. S. J. van der Zant, C. Dekker, L. P. Kouwenhoven, and S. De Franceschi, *Phys. Rev. Lett.* **94**, 156802 (2005).
- [5] A. K. Hüttel, G. A. Steele, B. Witkamp, M. Poot, L. P. Kouwenhoven, and H. S. J. van Zant, *Nano Lett.* **9**, 2547 (2009).
- [6] J. M. Kinaret, T. Nord, and S. Viefers, *Appl. Phys. Lett.* **82**, 1287 (2003).
- [7] P. Poncharal, Z. L. Wang, D. Ugarte, and W. A. de Heer, *Science* **283**, 1513 (1999).
- [8] L. D. Landau, *Phys. Z. Sowjetunion* **3**, 644 (1933); A. S. Alexandrov and N. F. Mott, *Polarons and Bipolarons* (World Scientific, Singapore, 1995).
- [9] M. Verissimo-Alves, R. B. Capaz, B. Koiller, E. Artacho, and H. Chacham, *Phys. Rev. Lett.* **86**, 3372 (2001); L. S. Brizhik, A. A. Eremko, B. M. A. G. Piette, and W. J. Zakrzewski, *J. Phys. Condens. Matter* **19**, 306205 (2007).
- [10] See Supplemental Material at <http://link.aps.org/supplemental/10.1103/PhysRevLett.108.076805> for additional detail regarding numerical methods and some calculations.
- [11] R. Tamura and M. Tsukada, *Phys. Rev. B* **52**, 6015 (1995).
- [12] T. Ando, *J. Phys. Soc. Jpn.* **74**, 777 (2005).
- [13] L. D. Landau and E. M. Lifshitz, *Theory of Elasticity* (Addison-Wesley, Reading, MA, 1959); M. Poot, B. Witkamp, M. A. Otte, and H. S. J. van Zant, *Phys. Status Solidi B* **244**, 4252 (2007).
- [14] A. Krishnan, E. Dujardin, T. W. Ebbesen, P. N. Yianilos, and M. M. J. Treacy, *Phys. Rev. B* **58**, 14013 (1998).